Gene 558 (2015) 54–64

AUTHOR'S ACCEPTED VERSION

Gene

Internal transcribed spacer (ITS) evolution in populations of the hyperparasitic European mistletoe pathogen fungus, *Sphaeropsis visci* (*Botryosphaeriaceae*): The utility of ITS2 secondary structures

Péter Poczai [a,*,1], Ildikó Varga [b,1], Jaakko Hyvönen [b]

[a] *Botany Unit, Finnish Museum of Natural History, University of Helsinki, PO Box 7, Helsinki FI-00014, Finland*
[b] *Plant Biology, Department of Biosciences, PO Box 65, FI-00014, University of Helsinki, Finland*

ARTICLE INFO

Article history:
Received 18 August 2014
Received in revised form 29 November 2014
Accepted 19 December 2014
Available online 20 December 2014

Keywords:
Ascomycetes
Internal transcribed spacer (ITS)
Hyperparasitism
Parasitic plants
Viscum album

ABSTRACT

We investigated patterns of nucleotide polymorphism in the internal transcribed spacer (ITS) region for *Sphaeropsis visci*, a hyperparasitic fungus that causes the leaf spot disease of the hemiparasite European mistletoe (*Viscum album*). Samples of *S. visci* were obtained from Hungary covering all major infected forest areas. For obtaining PCR products we used a fast and efficient direct PCR approach based on a high fidelity DNA polymerase. A total of 140 ITS sequences were subjected to an array of complementary sequence analyses, which included analyses of secondary structure stability, nucleotide polymorphism patterns, GC content, and presence of conserved motifs. Analysed sequences exhibited features of functional rRNAs. Overall, polymorphism was observed within less conserved motifs, such as loops and bulges, or, alternatively, as non-canonical G–U pairs within conserved regions of double stranded helices. The secondary structure of ITS2 provides new opportunities for obtaining further valuable information, which could be used in phylogenetic analyses, or at population level as demonstrated in our study. This is due to additional information provided by secondary structures and their models. The combined score matrix was used with the methods implemented in the programme 4SALE. Besides the pseudoprotein coding method of 4SALE, the molecular morphometric character coding also has potential for gaining further information for phylogenetic analyses based on the geometric features of the sub-structural elements of the ITS2 RNA transcript.

1. Introduction

Ribosomal RNA (rRNA) genes and their spacer regions have become widely used as a source of phylogenetic information across the entire breadth of life (Dixon and Hillis, 1993). The internal transcribed spacer (ITS) is intercalated in the 18S–5.8S–28S region, separating the elements of the rDNA locus. The ITS region consists of three parts: ITS1, ITS2 and the highly conserved 5.8S rDNA exon located between them. The internal transcribed spacer 2 (ITS2) region of nuclear ribosomal RNA has been proposed as one of the candidate DNA barcodes for fungi because it possesses a number of valuable characteristics (Yao et al., 2010). During molecular processes of ribosome maturation the entire rDNA region is transcribed as a single precursor rRNA and then goes through complex excision processes which affect both ITS regions (Pöll et al., 2009). The correct higher order structure of both spacers is important for directing endonucleolytic enzymes to the proper cut sites (Mai and Coleman, 1997). ITS2 usually has a conserved secondary structure with four helices which appear to be essential for successful excision of ITS2 from the precursor rRNA (Caisová et al., 2011). Modelling this clover leaf-like structure was recently proposed as a novel tool for phylogenetics (Wolf et al., 2005). This was based on phylogenetic inferences based not only on sequence information, but also on predicted secondary structures. The possibility to predict the folding structure has enhanced the role of ITS2 in phylogenetic studies, since it could lead to additional information. As summarized in Poczai and Hyvönen (2010), the variability in ITS2 is due to frequently occurring nucleotide polymorphisms or to common insertions/deletions in the sequence. This high rate of divergence is also an important source for studying population differentiation or phylogeography (Baldwin, 1993; Vargas et al., 1999; Yamaji et al., 2007). It has been widely utilized in studies of diverse organisms (Schultz et al., 2005; Keller et al., 2008; Yao et al., 2010), including fungi (Schoch et al., 2012).

Abbreviations: AIC, Akaike information criterion; diPCR, direct PCR; HMMs, Hidden Markov Models; ITS, internal transcribed spacer; MCP, phylogenetic dual multiple change-point model; PDA, potato dextrose agar; SIC, simple indel coding.

* Corresponding author.
E-mail addresses: peter.poczai@gmail.com (P. Poczai), ildikovarga@hotmail.hu (I. Varga), jaakko.hyvonen@helsinki.fi (J. Hyvönen).

[1] These authors contributed equally to this work.

http://dx.doi.org/10.1016/j.gene.2014.12.042
0378-1119/

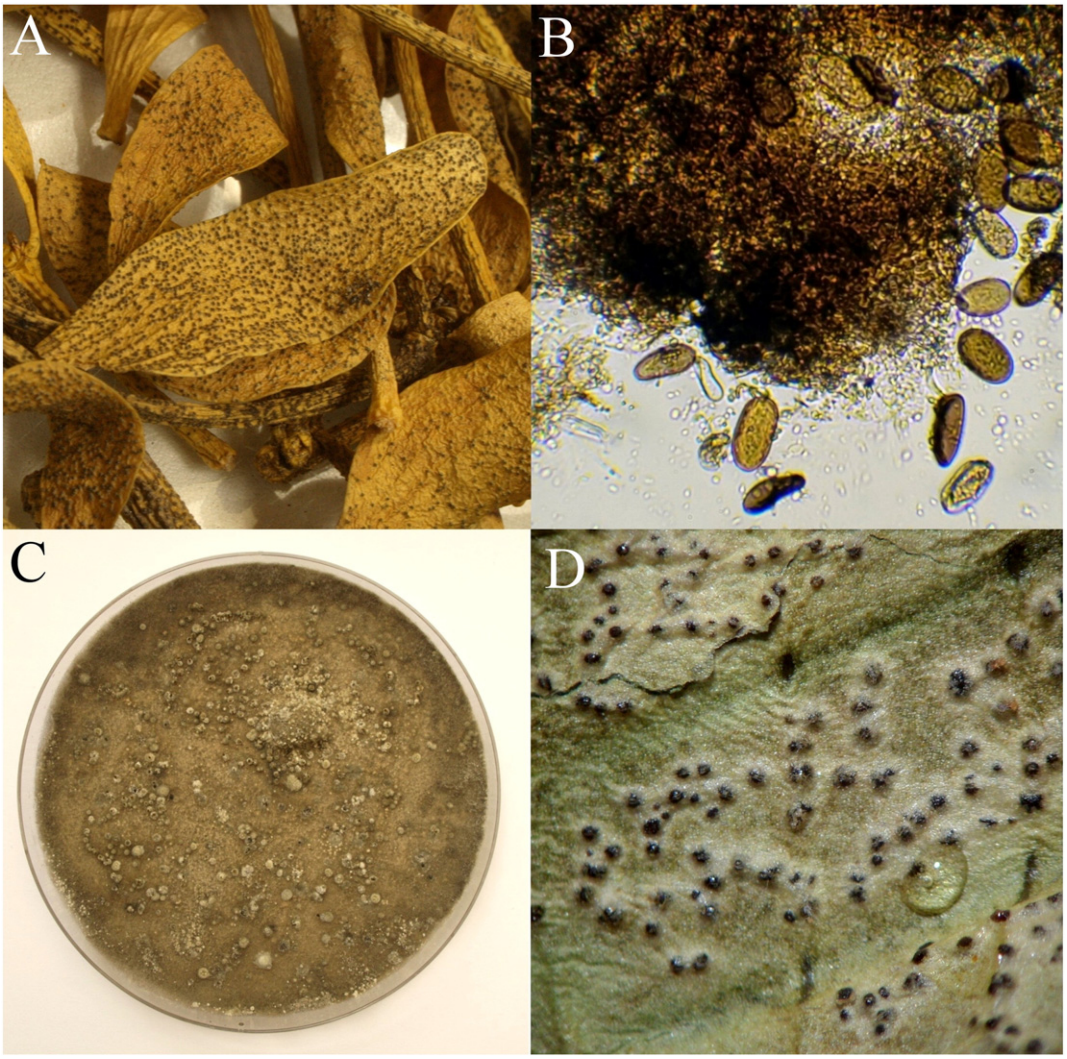

Fig. 1. Morphological features of the hyperparasitic mistletoe pathogen fungus (*Sphaeropsis visci*). A. Infected European mistletoe (*Viscum album*) twig showing yellow chlorotic symptoms caused by the hyperparasitic fungus. B. Moderately thick-walled, aseptate conidia bursting out from a pycnidium. Fine oil droplets and colour differences between young (greenish yellow) and older (dark brown) conidia are clearly visible. C. *Sphaeropsis visci* culture grown on media for 14 days. D. Immersed to erumpent and superficial pycnidia formed on leaves.

Sphaeropsis visci (Basionym: *Sphaeria atrovirens* var. *visci* Alb. & Schwein., Consp. fung. (Leipzig): 48. 1805. = *Phaeobotryosphaeria visci* (Kalchbr.) A.J.L. Phillips & Crous, Persoonia 21: 47. 2008, for synonyms see Phillips et al. (2013)) is a dark-spored ascomycete of the family *Botryosphaeriaceae* (Fig. 1). It causes the leaf spot disease of the European mistletoe (*Viscum album* L.) and seems to have a potential as a tool of biological control against this hemiparasite plant (Fischl, 1996; Karadžić et al., 2004; Varga et al., 2012). European mistletoe in the family Viscaceae (Santalaceae sensu lato; Nickrent et al., 2010) is an evergreen, perennial, epiphytic, hemiparasitic shrub with persistent haustoria penetrating its hosts (Zuber, 2004). It causes large economic losses in forestry and agriculture because infected wood becomes unsuitable for processing and infected trees are predisposed to other infections. Mistletoe increases tree mortality and contributes to forest decline (Tsopelas et al., 2004; Idžojtić et al., 2008). With global warming this could become a more serious problem of larger economic importance (Noetzli et al., 2003). Recent studies show that warning signs can already be seen in the saturation of the European forest biomass carbon sink (Ciais et al., 2008; Pan et al., 2011). This is due to decreasing stem increment rate and thus to the curbing of the sink, coupled with intensifying deforestation (Nabuurs et al., 2013). Forest policies and management strategies need revision if we want to sustain the sink.

Using *S. visci* as a mycopesticide against mistletoe would have many advantages. The fungal infections spread all over the leaves, branches and berries, causing the whole shrub to become dark yellow and necrotic within a few months. As well as being environmentally friendly, such a biological control method can be applied in places where pesticide spilling is impossible, e.g., in urban areas or next to kindergartens, or where mechanical removal is impractical. In order to develop *S. visci* as an effective bio-control agent against *V. album* more information will be needed about epidemiology, population biology and the distribution of possible haplotypes. Regarding the latter objective, identification of origin of samples using ITS region sequences is a useful tool, but limited numbers of *S. visci* isolates have been characterized. For example, ITS diversity may indicate a recent introduction and spread of this pathogen, whereas variability within small region may indicate that the species has already been in the area for some time, and that other factors such as management practices or environmental changes have been responsible for the apparent increase in infections.

Here we attempted to assess the diversity of the *S. visci* ITS region and to discover whether specific ITS2 secondary structures are found in the Hungarian population. We also aimed to study ITS region diversity from the isolates in order to develop a molecular based identification method and to obtain information about infraspecies diversity and evolution of *S. visci*.

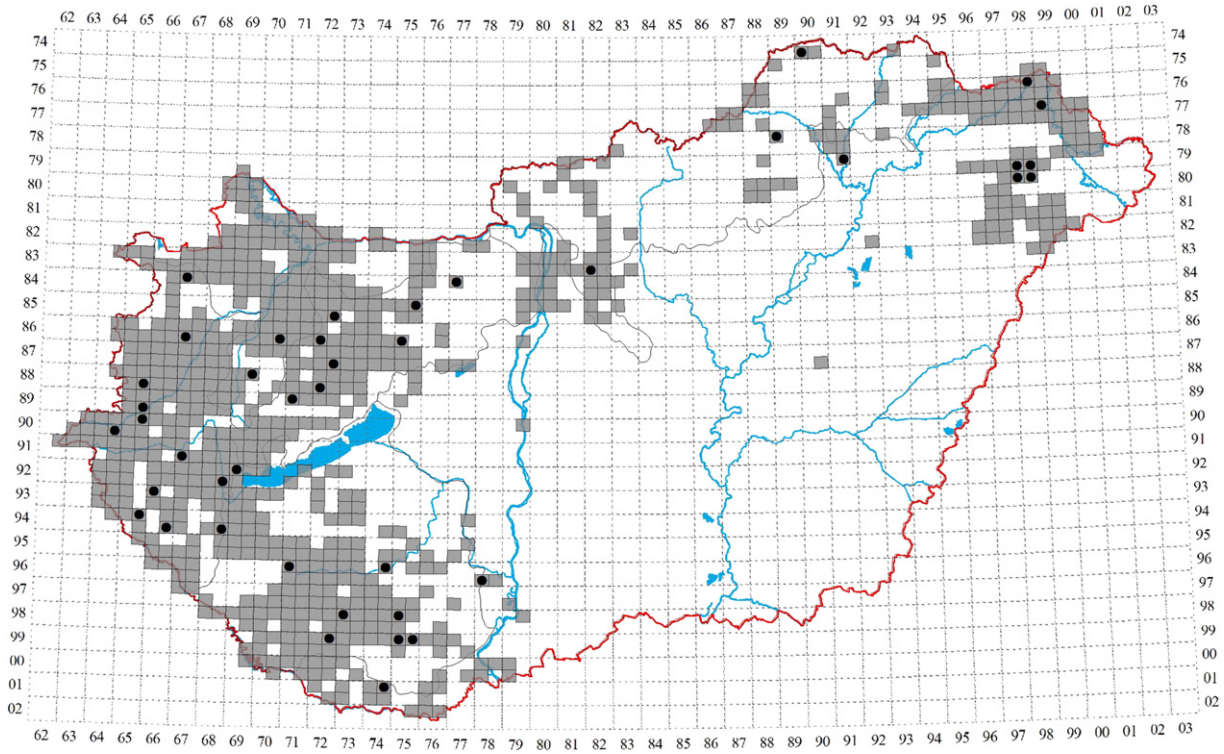

Fig. 2. The distribution of *Viscum album* in Hungary on a grid-cell map. Grey shaded grid-cells represent the occurrence of *Viscum album*, while black dots mark sampling sites of *Sphaeropsis visci*.

2. Materials and methods

2.1. Sample collection

Infected European mistletoe leaves were collected in 2010 and preserved as herbarium samples. No specific permissions were required for sampling at locations; our study did not involve endangered or protected species. GPS coordinates for each study site are provided as Supplementary data 1. Sampling sites and the distribution of *V. album* and *S. visci* are shown in Fig. 2. The distribution of this hyperparasitic fungus strongly depends on the limited occurrence of its hemiparasitic host (Varga, 2013). For this reason we attempted to collect samples on a region-wide basis rather than many samples from a single location. The occurrence of the fungus is also affected by complex environmental factors and correlates with the host (Varga, 2013). During our fieldwork we observed mass infections of the fungus in locations where the host trees were old or in relatively poor condition, as well as in areas where large numbers of individuals of the hemiparasitic host were found. The fungus was rare in isolated mistletoe populations. For these reasons it was not present in all regions, or else its distribution was limited which also affected our sampling. Sequences from pure culture reference strains deposited in MycoBank (Robert et al., 2005) and in GenBank (Benson et al., 2011) were also included in our analyses. Multiple outgroup terminals were chosen according to our previous morphological and molecular identifications (Varga et al., 2012) of the isolates and were selected from closely and more distantly related clades of the *Botryosphaeriaceae* following Phillips et al. (2008). These included the closely related taxa *Sphaeropsis citrigena* (AJL Phillips, PR Johnst. & Pennycook) AJL Phillips & A Alves, *Phaeobotryon mamane* Crous & AJL Phillips from the sister clade, *Botryosphaeria dothidea* (Moug.) Ces. & De Not. from the more basal lineage and one representative of the distantly related *Diplodia cupressi* AJL Phillips & A Alves from the same family.

2.2. Direct PCR, sequencing and cloning

Samples were separately placed into a wet-chamber and incubated for one day at 25 °C to swell the conidiomata. Thirty conidiomata were carefully excised from each leaf sample and suspended in 800 μl of sterile distilled water. From this suspension 250 μl triplicates were spread with a glass rod on streaking PDA plates (4 g potato extract, 20 g glucose, 15 g agar per litre). Petri-dishes were incubated at 25 °C for 24 h and then germinating spores were removed individually and placed on PDA plates containing 30 mg/l Kanamicyn and 100 mg/l Ampicillin. Monospore cultures were further incubated for 1 week at 25 °C. Final subcultures were made for DNA purification from disks 5 mm in diameter excised from the proliferation zone of the colonies, which were placed on a semi-permeable plastic membrane ensuring the isolation of mycelia. DNA was extracted from mycelia using the Phire Plant Direct PCR Kit (Thermo Fisher Scientific, USA) procedure. This tissue-direct technique requires very little sample material as compared to alternative methods. It provides fast and accurate processing of fungal samples in species identification and description (Zhou and Wei, 2012; Cao and Yuan, 2013) and has also been used in forensic studies (Gausterer et al., 2012). The excised small fungal samples were lysed in 20 μl dilution buffer and crushed with pipette tips in Eppendorf tubes. The samples were incubated at room temperature for 5 min, then 1 μl of the supernatant was used as template in the PCR amplification. The amplification was performed with the primers ITS1 (5′-TCCG TAGGTGAACCTGCGG-3′) and ITS4 (5′-TCCTCCGCTTATTGATATGC-3′) (White et al., 1990). We followed the protocol of the Phire Plant Direct PCR Kit (Thermo Fisher Scientific, USA) for amplification reactions, which were performed in 20 μl volumes containing: 7 μl nuclease free water, 0.6 μl sample (from dilution protocol), 0.5 μM of each primer, 10 μl 2 × Phire Plant PCR buffer and 0.4 μl of Phire Hot Start II DNA Polymerase (Thermo Fisher Scientific, USA). All PCR reactions were performed in the following conditions: 5 min at 98 °C for initial

denaturation, 40 cycles of 5 s denaturation at 98 °C, 5 s annealing at 54 °C, and 20 s extension at 72 °C, followed by a final extension for 1 min at 72 °C. Reactions were performed with the following cycling conditions: 5 min at 98 °C for initial denaturation, 40 cycles of 5 s denaturation at 98 °C, 5 s annealing at 54 °C, and 20 s extension at 72 °C, followed by a final extension for 1 min at 72 °C. Amplification products were separated on 1.5% agarose gels stained with ethidium-bromide. Clean up of PCR products was performed by removing non-incorporated primers with 10 U exonuclease I and degradation of nucleotides by 1 U thermosensitive alkaline phosphatise (Exo I and FastAP, Fermantas, Lithuania). PCR mixes were incubated at 37 °C for 15 min and the reaction was stopped by heating the mixture at 85 °C for 15 min. Fragments excised from agarose gels or direct PCR (diPCR) products were cleaned with the NucleoSpin Extract II Kit (Machery-Nagel, Germany) and cloned to JM107 competent *Escherichia coli* strains using the ColneJET PCR Cloning Kit (Fermentas, Lithuania) and the Transform Aid Bacterial Transformation Kit (Fermentas, Lithuania). The procedures were carried out according to the manufacturers' instructions. Plasmids were extracted from selected colonies holding the desired insert with the NucleoSpin Plasmid DNA Kit (Machery-Nagel, Germany). Direct and plasmid sequencing was performed with an ABI 3130XL automated sequencer in both directions using the ABI PRISM BigDye Terminator Cycle Sequencing Ready Reaction Kit v.3.0. All sequences were annotated and deposited in GenBank; accession numbers are available as Supplementary data 1.

2.3. Sequence assembly, alignment and indel coding

Forward and reverse sequence reads for all isolates were assembled with CodonCode Aligner v.3.7.1. (www.codoncode.org). Discrepancies were manually resolved by editing the traces using the compare option of the advanced assembly function. Single consensus sequences were exported in FASTA format from the assemblies. Multiple sequence assemblages were aligned with MUSCLE (Edgar, 2004) as implemented in Geneious v.4.8.5 (www.geneious.com/) using the default settings. Ribosomal exons and spacer regions were annotated in the alignments using the fungal reference sequences deposited in the ITS2 database (http://its2.bioapps.biozentrum.uni-wuerzburg.de/). This facilitated additional editing and processing of the sequences. Final data sets were formatted as NEXUS files using the export options of Geneious. Sequence statistics were calculated either with SeqState (Müller, 2005) or MEGA v5 (Tamura et al., 2011). Gaps (or 'indels') were utilized as an additional source of data for phylogenetic inference. These microstructural changes of the rRNA ITS region were coded as binary characters using the simple indel coding (SIC) method of Simmons and Ochoterena (2000) implemented in SeqState (Müller, 2005). The programme generates a ready-to-use NEXUS-file containing the binaries, which were further edited manually prior to analysis. This file containing the concatenated binaries is provided as Supplementary data 2.

2.4. Analysis of ITS2 secondary structure

2.4.1. Structure reconstruction

For further analyses, ITS2 sequences were extracted from the alignment between the 5.8S and 28S proximal stem motifs. The hybridization of these regions was visually checked using the ITS2 database III (Koetschan et al., 2010) and the 'Annotate' function implementing Hidden Markov Models (HMMs) (Keller et al., 2009). For folding we used an E-value < 0.001 and fungi HMMs with ITS2 minimum size 150 nt< in order to define the borders of ITS2. Incorrect folding of this region can be a good indicator of the presence of pseudogenes (Harpke and Peterson, 2008a). ITS2 secondary structures were reconstructed using the 'Predict' function of the ITS2 database Beta version applying a 75% threshold level for helix transfer. This method was developed by Schultz et al. (2006) to predict ITS2 structures and is based on the Needleman and Wunsch (1970) algorithm, additionally applying a BLAST search of the database with the newly predicted structure in order to compare it to others. Results were converted to FASTA files containing the models and sequences as parenthetical notations. The structures and sequences were synchronously aligned by 4SALE (Seibel et al., 2006) using only locally implemented alignment methods based on ClustalW (Larkin et al., 2007). The resulting structures were visualized with PseudoViewer3 (Byun and Han, 2009).

2.4.2. Molecular morphometric character coding

We considered the structures of the ITS2 RNA transcripts as phylogenetic characters useful for tree reconstructions. Two kinds of attributes were coded in our study relating to ITS2 structures; the geometrical features of the molecules described by such sub-structural elements as loops, stems and bulges, and a different approach in which the stability and uniqueness of the RNA molecules were represented. These characters were coded into a multistate format in the same manner as morphological traits used in phylogenetic inferences. Such characters describe the morphospace of specific molecules, providing a global description of elements found in the folded secondary structures. Shannon entropy of the base pairing probability matrix (Q), Frobenius norm values (F), base-pairing propensity (P) and mean stem length were used to describe statistical features of the structures. The utility of these statistics has been previously demonstrated (Harish and Caetano-Anollés, 2012). For all calculations we used the web interface of STOAT implemented on the NOBAI web server (Knudsen and Caetano-Anollés, 2008). We used previously predicted ITS2 structures as input data together with primary sequences in FASTA format read directly by STOAT.

Characters describing the shapes of the molecules were generated by the programme 4SALE, which applies a unique method to simultaneously align structure-sequence data by translating it into a 12 letter pseudoprotein format, which incorporates nucleotides and their possible states of being involved in secondary structure formation (Seibel et al., 2008).

2.5. Phylogenetic analysis

2.5.1. Bayesian analysis

Bayesian analysis was performed with MrBayes v3.2 (Ronquist et al., 2012). The dataset was divided into the following partitions: indel characters, molecular morphometric traits, and ITS2 secondary structure data in pseudoprotein format from 4SALE. DNA sequence characters were further divided into 18S, ITS1, 5.8S, ITS2 and 28S partitions, respectively. The best-fit nucleotide substitution models for each DNA partition were selected with jModelTest 2 (Darriba et al., 2012) using the Akaike information criterion AIC (Akaike, 1974). The HKY model (Hasegawa et al., 1985) was assigned to ITS1, 5.8S, ITS2 and 28S. We applied $nst = 1$ in MrBayes for the 18S partition constraining a model where all of the rates are the same (F81). The restriction site model was applied for the binary indel partition while ITS2 molecular morphometric characters were analysed as 'standard'. For the 4 SALE pseudoprotein data we applied the Blossum protein evolution model selected with ProtTest (Abascal et al., 2005). We unlinked all parameters across partitions in the command file. We attempted to sample all trees having a reasonable probability given the assembled datasets using the Metropolis-coupled Markov chain Monte Carlo $(MC)^3$ method. For this reason we kept all sequences in the alignments even if they were identical (based on population genetic assumptions, i.e., not misleading the BI by assuming a larger population). Several initial shorter runs with only four chains were performed to fine-tune the parameters and assess appropriate mixing. Further analyses were initiated with four runs and eight chains (10^6 generations each). We sampled every 1000th generation to reduce the size of output files and make the samples more independent. Analyses were performed using the mainframe computers of the CSC — IT Center for Science (www.csc.fi), Espoo, Finland by assigning each chain to a separate CPU. Simulations were run until stationarity was reached as assessed by average standard

deviations of split frequencies < 0.01. MC^3 convergence was explored by examining the Potential Scale Reduction Factor (PSRF) for all parameters in the model and plots of log-likelihoods over time together with other plots for all parameters viewed in Tracer v1.4 (Rambaut and Drummond, 2012). Additional tests of convergence were conducted with the online programme AWTY (Nylander et al., 2008) using the 'cumulative' and 'compare' functions and with 25% burn-in. Trees from BI analyses were summarized as majority-rule consensus trees and edited with TreeGraph2 (Stöver and Müller, 2010). The final assembled concatenated data matrix is available as Supplementary data 3.

2.5.2. Parsimony analysis

Before performing maximum parsimony phylogenetic analysis we were able to reduce the size of the matrix to include only 40 terminals, due to numerous, completely identical terminals. The list of identical and deleted sequences is provided in Supplementary data 4. Using the WinClada (Nixon, 2002) command "Mop uninformative characters" we reduced our matrix to 40 × 100 characters. Due to this small effective size the most efficient way to implement parsimony analysis was by using Nona (Goloboff, 1994) within the WinClada shell. We performed analyses (using processor time as a seed to randomize the order of the terminals) with the following settings: hold 3000 (holding a defined number of trees), 100 replications (search performed with multiple tree–bisection–reconnection algorithm iterations mult*max*), and hold/20 (keeping twenty starting trees for each replication). In addition we performed a larger analysis holding up to 30,000 trees (hold 30,000), but keeping only two starting trees for each replication (hold/2). Jackknife support values were calculated using 1000 replications, with 10 search replications (multi*10) and three starting trees per replication (hold/3).

2.6. Recombination detection

We tested for recombination using a Bayesian multiple change point model, DualBrothers (Minin et al., 2005), as implemented in the software package Geneious. Default settings were used with the following exceptions: chain length was set at 220,000, subsampling frequency at 100 and burn-in length at 10,000. DualBrothers is a recombination detection algorithm based on a phylogenetic dual multiple change-point model (MCP) (Suchard et al., 2003). The MCP model allows for changes in evolutionary relationships and rates across sites in a multiple sequence alignment by assuming that the sites separate into an unknown number of contiguous segments, each with possibly different topologies or mutation processes (McBride et al., 2009).

3. Results

3.1. Phylogenetic analysis

To determine evolutionary relationships among the isolates we constructed phylogenetic trees based on the complete sequence of the rRNA ITS region and using the indels found in this region as binary characters concatenated with RNA secondary structure data obtained for ITS2. Ancestral haplotypes were identified by parsimony and Bayesian analyses. Both parsimony analyses resulted in the same set of 96 equally parsimonious trees with a length of 199 steps (the consensus of these illustrated in Fig. 3). Consistency (CI; Kluge and Farris, 1969) and retention indices (RI; Farris, 1989) were 0.61 and 0.64, respectively. The results of the two Bayesian runs conducted with MrBayes were highly congruent with each other. PSRF values averaged 1.0000–1.0001 strongly suggesting that stationarity had been reached. Comparison of the topologies and associated posterior probability values obtained across the independent runs for the dataset with AWTY verified convergence. Inspection of the log likelihood trace plots and comparison of these for the two runs also indicated that the runs had reached stationarity. Runs reached stationarity after 8×10^5 generations. The

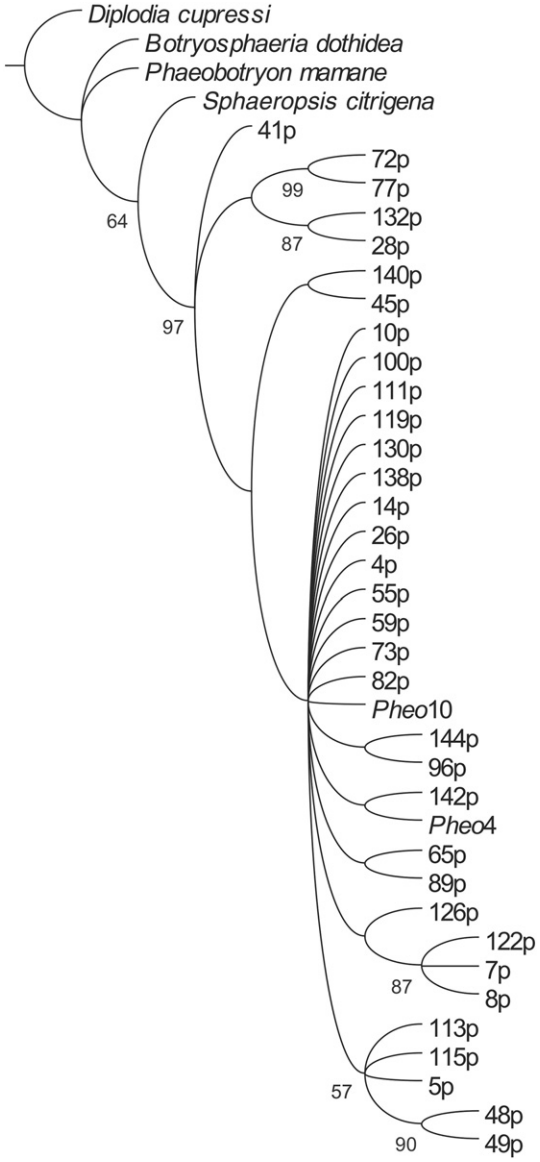

Fig. 3. The consensus tree inferred from the parsimony analyses of the ITS region. Identical terminals were removed, numbers beside clades indicate jackknife support values.

Bayesian majority rule consensus tree and a phylogram are illustrated in Fig. 4.

Both Bayesian and parsimony analyses strongly supported a separate clade composed exclusively of *S. visci* isolates. Branch lengths on phylogenetic trees indicated low levels of genetic variation among the isolates. Closer inspection of the aligned sequences revealed only a limited number of single nucleotide polymorphisms (SNPs) among the terminals. These small differences may be attributable to topological differences among the phylogenetic trees. In the Bayesian analysis internal groups were unresolved on the majority rule consensus tree as the posterior probabilities of these clades were weak. The detected SNPs were not informative enough to separate them with high PP values.

3.2. Sequence variation of the complete rDNA ITS region

The complete rRNA ITS dataset showed variation in both length and nucleotide composition. For the analysed terminals the combined data matrix, consisting of the internal transcribed spacer 1 (ITS1, 154–200 bp), the 5.8S ribosomal gene (155 bp), the internal transcribed spacer 2 (ITS2, 149–169 bp), and partial sequences of the adjacent 18S and 28S genes, included a total of 661 characters.

Calculated sequence statistics are summarized in Table 1. The ITS1 region contained more variation (22.36%) than the ITS2 (15.69%) and 5.8S regions (6.45%). In the complete alignment 45 of the total 95 variable characters turned out to be parsimony informative. Both spacers had GC contents above 50%, while this value was below 50% for 5.8S. The average ratio of transitions to transversions (ti:tv) was 0.79 for the entire region. The two spacers had higher ti: tv ratios compared to the 5.8S gene (0.23), while ITS1 had the highest value (0.74). The ratios as a whole showed a bias towards transversional substitutions, which were more frequent. We also conducted a search to find putative repeats and forward/reverse motifs using Phobos as implemented within Geneious, which resulted in the discovery of a 7-nucleotid (CCCCGCG) repeat in aligned positions 159 to 198; a hexanucleotid (ACGTAG) repeat spanning from 156 to 167 and a tetranucleotid (AAAT) repeat from 268 to 278 in the ITS1 region. These findings suggest that the presence of smaller indels, rather than tandem repeats, plays the most important role in the observed length variation among *S. visci* isolates.

Table 1
Sequence statistics from the nuclear ribosomal ITS region. Sequence statistics for the entire rDNA internal transcribed spacer region based on the total aligned dataset including outgroup terminals.

	ITS1	5.8S	ITS2	Total[a]
Sequence length range (bp)	154–200	155	149–169	520–606
Average length (SD)	157 (4.28)	155*	161 (1.81)	560 (5.71)
Aligned length	246	155	172	661
Variable characters (%)	55 (22.36)	10 (6.45)	27 (15.69)	95 (14.37)
PI characters[b]	28	3	11	45
Conserved sites	119	145	143	492
GC content (%)	56.71	47.07	59.56	53.71
ti: tv[c] (S.E.[+])	0.74 (0.41)	0.23*	0.53 (0.49)	0.79 (0.12)

[a] Total aligned sequences with partial sequences of 18S and 28S ribosomal genes, which may include additional conserved/variable characters.
[b] PI = parsimony informative characters.
[c] Transition/transversion ratio.
[+] Standard errors calculated based on 1000 bootstrap replicates.
* Standard error is 0.0001<.

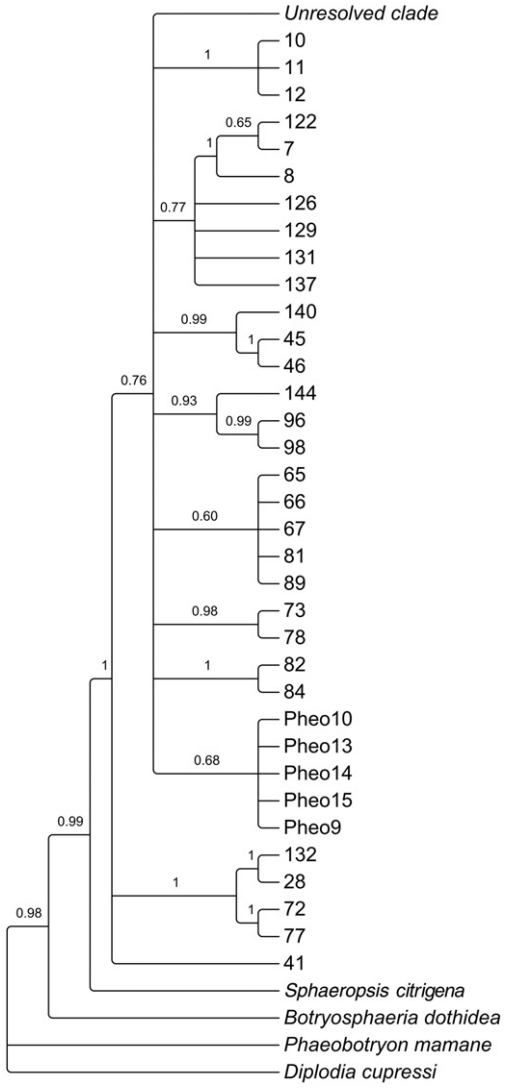

Fig. 4. The majority rule consensus tree of the Bayesian analyses of the ITS region. Identical terminals were removed, numbers above branches represent posterior probability (PP) values. The unresolved clade mostly encompasses isolates with ITS2α but ITS2γ types are also found in this group. Isolates in the unresolved clade are: 3, 4, 6, 14–22, 25–27, 29–40, 42, 44, 47, 50–56, 58, 59, 60, 62–64, 68–71, 74–76, 79, 80, 86, 91–94, 99, 100–113, 114, 116, 117, 119–121, 123–125, 127, 130, 133–135, 138–139, 141, 144, Pheo1-3, Pheo5-8, Pheo11-19.

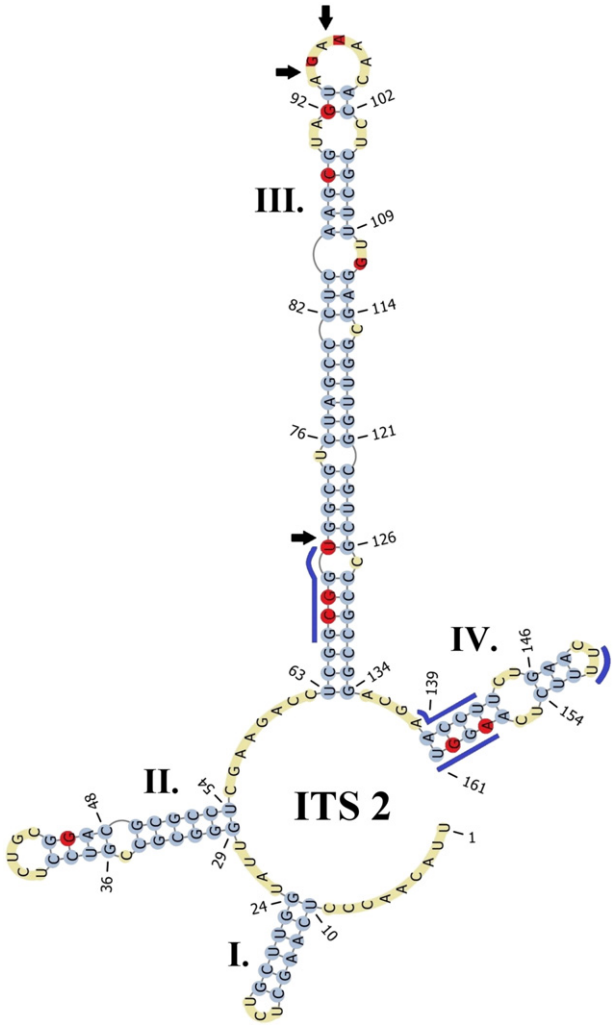

Fig. 5. Structural features of the ITS2 in *Sphaeropsis visci*. General topology of the common ITS2 secondary structure of *Sphaeropsis visci* with annotated features of structure differences found among the sampled populations. The four helices appearing in the reconstructions are subsequently numbered with capital roman number. Numbering of the bases starts from the 5′ and end at the 3′. Unpaired nucleotides forming pseudoknots are coloured beige; paired nucleotides forming the helices are shown in blue, while variable positions in within isolates are highlighted in red. These positions were identified via 4SALE local alignment. Blue lanes indicate deletions while black arrows point to the position of insertions among isolates.

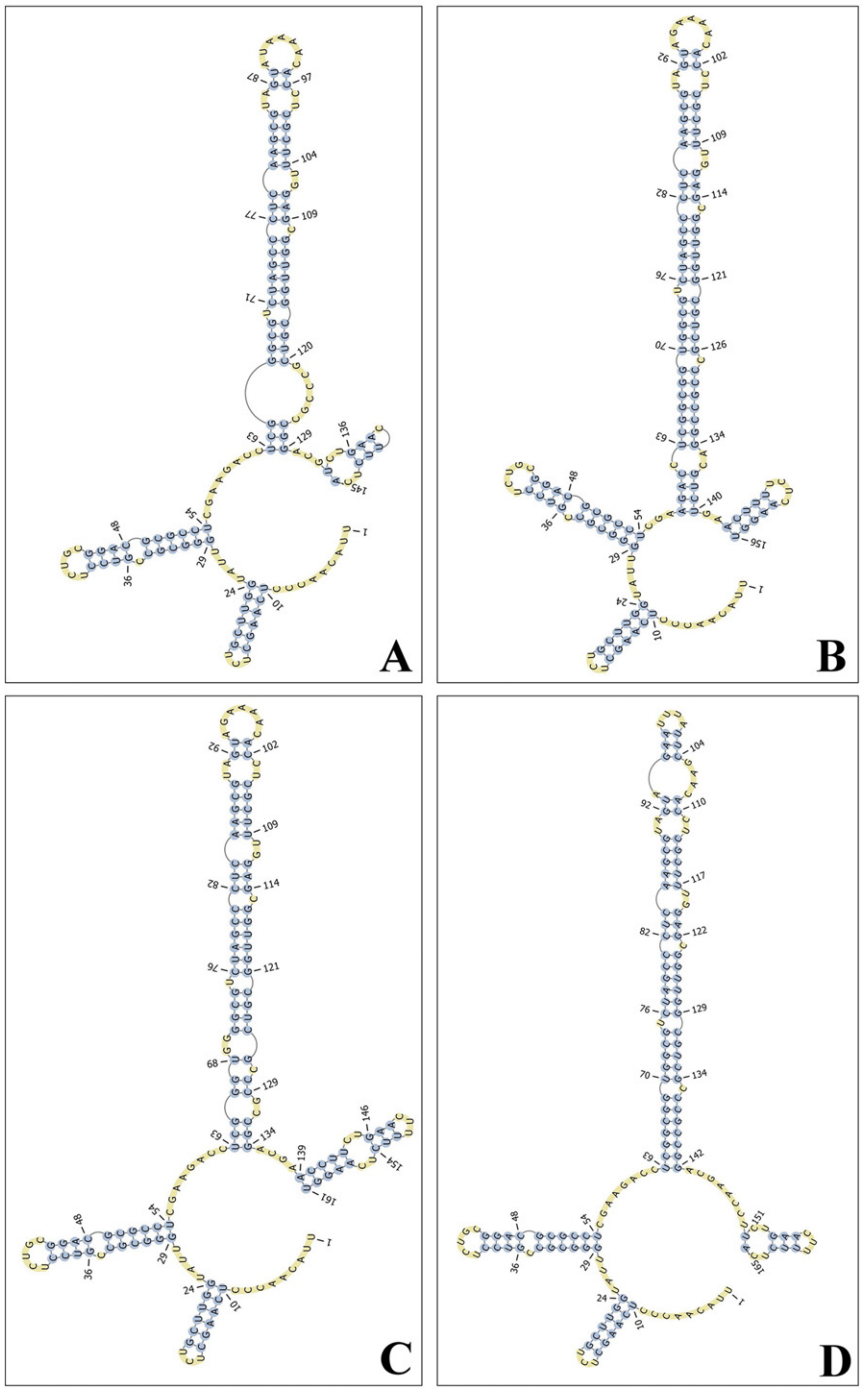

Fig. 6. Secondary structure of different ITS2 types found in populations of *Sphaeropsis visci*. Modified structures for ITS2β to ε are shown and number alphabetical order A to D.

3.3. Characteristics of the ITS2 secondary structure

The ITS2 secondary structure of *S. visci* isolates consists of four helices with the third forming the longest arm. The 4SALE alignment resulted in a 51% consensus sequence where the conservation of single base pairs varied from 90% to 100%, creating a robust structure. Single nucleotide polymorphisms (SNPs) occurred most frequently in helices III and IV, as did indels. However, one SNP was also found in helix II. The identified SNPs did not induce any further compensatory base changes (CBCs) or hemi-CBCs according to further checking by 4SALE. These specific polymorphisms of the primary RNA transcript maintaining paired sites during mutation events were also lacking in the outgroup taxa. We identified a common ITS2 structure typical for most of the isolates, defined as the ITS2α type. The structure of this common type with further annotations for variations occurring among the isolates is shown in Fig. 5. The synchronous alignment of sequence-structure data revealed variation missed by conventional MUSCLE alignment and allowed four alternative ITS2 indel structure forms occurring in *S. visci* populations to be distinguished (Fig. 6), subsequently labelled with Greek letters (ITS2β–ε). The ITS2β type was found in isolates 28, 82, 84 and has a characteristic AACCU deletion at aligned positions 147–151 in helix IV according to the 4SALE sequence-structure

alignment (see Supplementary data 5). This has resulted in the shortening of the fourth helical arm due to the disappearance of the unpaired CU–CU region and the formation of an additional C–CA bulge in helix III (Fig. 6a). The ITS2γ type (isolates 5, 83, 113, 115) has two insertions in helix III at aligned positions 96–100 (GAAU) and 103–105 (UUC). These have resulted in the extension of the helix III tip, forming a new terminal loop, and the shortening of helix IV. A two base pair deletion (aligned positions 66–67 CG) and an insertion of the same length (70–71 GG) also occurring in helix III characterizes the ITS2δ type (isolates 45, 46). These two simple changes have induced two additional bulges bordering the small C bulge near the base of helix III. The shortest and rarest structure was the ITS2ε type, which occurs only in isolate 140. It has accumulated many deletions in helix III (66–70 GCGGU) and helix IV (147–151 AACCU; 159–160 UU; 167–170 AGGU). These have shortened the fourth helical arm, inducing a larger loop in helix III. The SNPs occurring in the ITS2 region represent a shift towards transversions, with five T ↔ G changes and two C → G plus one A → C change. Transitions included only the interchange of two-ring purines (A ↔ G) in three cases.

4. Discussion

4.1. Utility of ITS2 structures in genetic diversity analysis

We focused on the potential of ITS2 to discriminate among the populations of *S. visci*. To identify and group the isolates, we used not only the divergence of primary sequences of ITS2, but also variations found in its secondary structure. We recommend including sequence and secondary structure information together for future studies aiming the study of lower level evolution and infraspecific genetic diversity. The combination and simultaneous analysis of sequence and structural ITS2 RNA data supplemented with indel coding binaries yielded robust phylogenetic hypotheses as measured by bootstrap values for ancestral haplotypes. However, the infraspecific variation observed in ITS2 structures was smaller within the populations as compared to the interspecific differences when outgroups were also considered.

Next generation sequencing technologies (NGS) have enabled the assembly of large datasets for plant pathogen populations. Such datasets are useful for investigating the distribution patterns of evolutionary constrains, for example in the ITS region within a given species (Freire et al., 2012). As experimental errors cannot be completely avoided, secondary structure modelling may assist in revealing erroneous polymorphisms, as was also emphasized by Freire et al. (2012). This is based on the observation that double stranded helices and hairpin stems accumulate much fewer nucleotide changes than loops and bulges, which are less important in maintaining the functional secondary structure (Poczai and Hyvönen, 2010). It seems that different taxonomic levels show different levels of similarity and variation in secondary structures (Schultz et al., 2005). In our study helices III and IV were the most variable regions. This is consistent with the results of previous studies where it was found that among eukaryotes, nucleotide sequences evolve most rapidly in region IV (Coleman, 2003). Also, the 5′ section near the tip of helix III was highly conserved here and included a UGAU motif, similar to the UGGU motif found in angiosperms. It has also been suggested that helix II is more stable (Koetschan et al., 2010), and this was the case in our study. The single stranded ring of the four-fingered model between helices I and IV was very conserved among the isolates and rich in purine nucleobases. The overall result of these molecular processes is that ~139 bases are conserved in *P. visci* populations. The remaining regions that are not necessary for the ribosome biogenesis machinery were variable enough to characterize the isolates. Therefore, close inspection of the distribution of mutations in the structure of ITS2 could facilitate the discrimination of true and artefactual polymorphisms.

4.2. The formation of different ITS2 types: pseudogenes or functional paralogs?

In population genetic studies direct sequencing could be a source of error that is mistakenly interpreted as natural sequence variation. For this reason we attempted to obtain PCR products and sequences with as few errors and false polymorphisms as possible using a fast and accurate method and by molecular cloning. This was possible partially because we used a high fidelity DNA polymerase with about 50 times greater fidelity than the conventionally used *Taq* DNA polymerase (Frey and Suppmann, 1995). This may suggest that structural and DNA polymorphisms found are likely to be due to natural sequence variation in *S. visci* and not false artefactual variation. It is also important to distinguish between sequences generated from pseudogenic and from functional rDNA loci for phylogenetic and population genetic studies. To achieve this we analysed the hybridization model of the 5.8S–28S rRNA proximal stem. The structure of this region is of major importance in a functional ribosomal system (Venema and Tollervey, 1995), since in three dimensional space these free nucleotides are located on the same side of the helical arm (Keller et al., 2009), and any deviation from this structure is a reliable sign of the presence of pseudogenes (Harpke and Peterson, 2008b). However, deviations have been reported in rare cases (Keller et al., 2009). In our study all hybridization models of the *S. visci* 5.8S–28S rRNA proximal stem had a free nucleotide on each side with typically six bases between, indicating that amplicons are generated from functional ribosomal regions (Fig. 7). All sequences generated for this study passed this initial test with correct folding.

Besides the hybridization model of the 5.8S–28S rRNA proximal stem the GC content of the 5.8S gene itself could also be a good indicator of pseudogenes (Hershkovitz et al., 1999). Pseudogenes tend to have a lower GC content resulting from methylation related substitution, which can lead to loss of gene function (Poczai and Hyvönen, 2010). Li et al. (2013) suggested that in fungi, values range from 44% to 54% in functional copies. We also compared the GC content of 5.8S genes

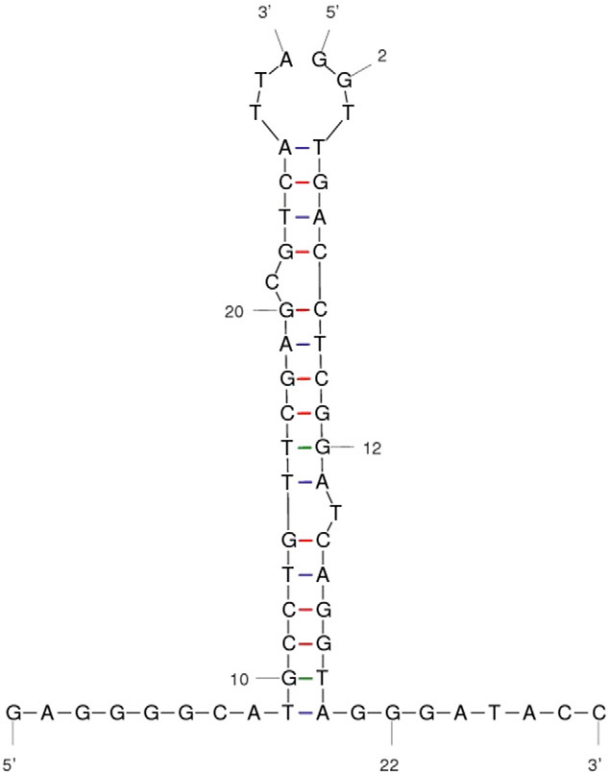

Fig. 7. Typical hybridization of the proximal stem. The nucleotides corresponding to the 5.8S are shown on the left while 28S are shown on the right. The proximal stem of the ITS2 is imperfect with one free nucleotide on each of the complementary strands.

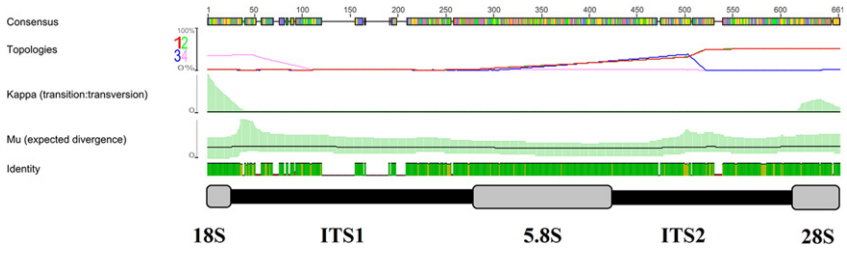

Fig. 8. Recombination detection graphs from the DualBrothers analysis. The analysis is based on the multiple change-point (MCP) model among aligned nucleotide sequences of the complete internal transcribed spacer region of the investigated *Sphaeropsis visci*. Bases represented by *coloured* boxes represent polymorphic sites. Signs of possible recombination events are represented as changes in the topology graphs (first row) that appear at the most probable topology between the segments. Higher slopes in the μ graph are indicators of regions which are affected by recombination in the ITS1 and ITS2 regions. The cross of the topological lines indicates recombination breakpoints.

from different ITS2 types, these varying from 44.1% to 47.1% and thus showing only slight differences. Additionally, we compared the secondary structure of the 5.8S genes as evolutionary constrains can be detected using low energy models (Mai and Coleman, 1997). The secondary structure stability of the 5.8S region has an important function in post-transcriptional processes, thus lower values for stability can also indicate the presence of pseudogenes. However, we only found minor, non-significant differences in free energy values (data not shown). Hence our secondary structure analyses of 5.8S suggest that the ITS2 types represent authentic gene copies, while GC content of 5.8S and bordering sequences also support the conclusion that they are not artefacts or of pseudogenic origin.

An alternative explanation for the occurrence of different ITS2 types could be that they have originated from paralogous loci that have escaped concerted evolution. Intragenomic variation, such as the existence of multiple paralogous or non-orthologous ITS copies, has been reported within single fruiting bodies of basidiomycetes (Smith et al., 2007; Lindner and Banik, 2011) and ascomycetes (Kovács et al., 2011), and also within axenic cultures (O'Donnell and Cigelnik, 1997). Contrary to frequently occurring intragenomic ITS variation in plants, relatively few intrasporocarpic ITS studies have been performed in fungi to examine intra-individual variability (Kovács et al., 2011). Some studies suggest that the process of concerted evolution is highly effective in homogenizing rDNA repeats in fungi (Ganley and Kobayashi, 2007). However, other studies have found intraspecific (Murat et al., 2004; Carriconde et al., 2008) or intagenomic/hyphal/sporocarpic variation (Kauserund and Schumacher, 2003; Avis et al., 2006) in ITS, and it has been hypothesized that such variation may be more frequent than has previously been thought (Simon and Weiss, 2008). In case of *S. visci* we used the asexual fruiting bodies (pycnidia) for the analysis of ITS variation. Different ITS2 types were found in rare cases, but detailed cloning shows that these variants are consistently found within an isolate. We found no mixed ITS2 types within pycnidia, just one dominant type, suggesting that they may not originate from paralogous loci.

4.3. Recombinations in the internal transcribed spacer region

Besides sexual recombination, several asexual processes may increase genetic diversity in fungi (Bolton et al., 2012). These include vegetative compatibility, parasexual recombination and mutation (Forgan et al., 2007; Bolton et al., 2012). *S. visci* is a hyperparasitic pathogen with reported anamorphic reproducing affinity (Phillips et al., 2008). However, very little is known about the reproductive biology of this pathogen. Teleomorphs of the species are rarely found, and the connection between *P. visci* and its anamorph *S. visci* was only recently demonstrated (Phillips et al., 2008). Our phylogenetic analysis reveals that the majority of isolates in our study occur in the same group as strains reported in previous studies (Phillips et al., 2008; Varga et al., 2012), indicating that there is a widely distributed ITS2 type (α) that is predominant in *S. visci* populations in Hungary. This has a common ITS sequence that matches sequences currently known from other countries in Europe (Phillips et al., 2008). The presence of different ITS types in the population could be attributed to sexual recombination or to the occurrence of teleomorphs, as shown by Ahvenniemi et al. (2009) for *Rhizoctonia solani*. We carried out recombination tests using a phylogenetic dual multiple change-point model (Fig. 8). This method assumes that evolutionary processes are not independent and identically distributed at each sequence site, which would produce spatial phylogenetic variation along the sequences. The model partitions the alignment into an arbitrary number of segments. When appropriate sequences representing the parental sequence are included, the topology describing a putative recombination can vary, with this appearing as variation in the most probable topology between the segments. Signs of recombination were detected with DualBrothers in certain parts of the ITS region, coinciding with the ITS2 sites marked on Fig. 8 and with areas of substantial polymorphism in the ITS1 region. However, during our large-scale field survey conducted in Hungary during 2010 (Varga et al., 2014) we were unable to find teleomorphs on *V. album* hosts (Varga, 2013). Clonality of the life cycle in this species has obviously reduced variation in the analysed population, although variation may be greater among populations if migration is rare. In the absence of gene flow, local selective sweep will remove variation within populations but not between populations. This should be investigated in detail with further large scale analyses sequencing more molecular markers. Analysis of the population genetic structure of this hyperparasitic fungus is currently underway and will be crucial for understanding the dynamics of such pathosystems.

Supplementary data to this article can be found online at http://dx.doi.org/10.1016/j.gene.2014.12.042.

Conflict of interest

The authors declare that they have no conflict of interest.

Acknowledgments

Thanks are due to Jari PT Valkonen for the comments made on the manuscript and to Neil Bell for the linguistic correction.

References

Abascal, F., Zardoya, R., Posada, D., 2005. ProtTest: selection of best-fit models of protein evolution. Bioinformatics 21, 2104–2105.
Ahvenniemi, P., Wolf, M., Lehtonen, M.J., Wilson, P., German-Kinnari, M., Valkonen, J.P.T., 2009. Evolutionary diversification indicated by compensatory base changes in ITS2 secondary structures in a complex fungal species, *Rhizoctonia solani*. J. Mol. Evol. 69, 150–163.
Akaike, H., 1974. A new look at the statistical model identification. IEEE Trans. Autom. Control 19, 716–723.
Avis, P.G., Dickie, I.A., Mueller, G.M., 2006. A 'dirty' business: testing the limitations of terminal restriction fragment length polymorphism (TRFLP) analysis of soil fungi. Mol. Ecol. 15, 873–882.
Baldwin, B.G., 1993. Molecular phylogenetics of *Calycadenia* (Compositae) based on ITS sequences of nuclear ribosomal DNA: chromosomal and morphological evolution re-examined. Am. J. Bot. 80, 222–238.
Benson, D.A., Karsch-Mizrachi, I., Lipman, D.J., Ostell, J., Sayers, E.W., 2011. GenBank. Nucleic Acids Res. 39, D32–D37.

Bolton, M.D., Secor, G.A., Rivera, V., Weiland, J.J., Rudolph, K., Birla, K., Rengifo, J., Campbell, L.G., 2012. Evaluation of the potential for sexual reproduction in field populations of *Cercospora beticola* from USA. Fungal Biol. 116, 511–521.

Byun, Y., Han, K., 2009. PseudoViewer3: general planar drawings of large-scale RNA structures with pseudoknots. Bioinformatics 25, 1435–1437.

Caisová, L., Marin, B., Melkonian, M., 2011. A close-up view on ITS2 evolution and speciation — a case study in the Ulvophyceae (Chlorophyta, Viridiplantae). BMC Evol. Biol. 11, 262.

Cao, Y., Yuan, H.-S., 2013. *Ganoderma mutabile* sp. nov. from southwestern china based on morphological and molecular data. Mycol. Prog. 12, 121–126.

Carriconde, F., Gardes, M., Jargeat, P., Heilmann-Clausen, J., Mouhamadou, B., Gyrata, H., 2008. Population evidence of cryptic species and geographical structure in the cosmopolitan ectomycorrhizal fungus, *Tricholoma scalpturatum*. Microb. Ecol. 56, 513–524.

Ciais, P., Schelhaas, M.J., Zaehle, S., Piao, S.L., Cescatti, A., Liski, J., Luysaert, S., Le-Maire, G., Schulze, E.-D., Bouriaud, O., Freibauer, A., Valentini, R., Nabuurs, G.J., 2008. Carbon accumulation in European forests. Nat. Geosci. 1, 425–429.

Coleman, A.W., 2003. ITS2 is a double-edged tool for eukaryote evolutionary comparisons. Trends Genet. 19, 370–375.

Darriba, D., Taboada, G.L., Doallo, R., Posada, D., 2012. jModelTest 2: more models, new heuristics and parallel computing. Nat. Methods 9, 772.

Dixon, M.T., Hillis, D.M., 1993. Ribosomal RNA secondary structure: compensatory mutations and implications for phylogenetic analysis. Mol. Biol. Evol. 10, 256–267.

Edgar, R.C., 2004. MUSCLE: Multiple sequence alignment with high accuracy and high throughput. Nucleic Acids Res. 32, 1792–1797.

Farris, J.S., 1989. The retention index and homoplasy excess. Syst. Zool. 38, 406–407.

Fischl, G., 1996. The leaf-spot disease of mistletoe (*Viscum album* L.). Növényvédelem 32, 181–183.

Forgan, A.H., Knogge, W., Anderson, P.A., 2007. Asexual genetic exchange in the barley pathogen *Rhynchosporium secalis*. Phytopathology 97, 650–654.

Freire, M.C.M., da Silva, M.R., Zhang, X.C., Almeida, A.M.R., Stacey, G., de Oliveira, L.O., 2012. Nucleotide polymorphism in the 5.8S nrDNA gene and internal transcribed spacers in *Phakospora pachyrhizi* viewed from structural models. Fungal Genet. Biol. 49, 95–100.

Frey, B., Suppmann, B., 1995. Demonstration of the Expand PCR System's greater fidelity and higher yields with lacI-based PCR fidelity assay. Biochemica 2, 34–35.

Ganley, A.R.D., Kobayashi, T., 2007. Highly efficient concerted evolution in the ribosomal DNA repeats: total rDNA repeat variation revealed by whole genome shotgun sequence data. Genome Res. 17, 184–191.

Gausterer, C., Stein, C., Stimpfl, T., 2012. Application of direct PCR in a forensic case of yew poisoning. Int. J. Legal Med. 126, 315–319.

Goloboff, P.A., 1994. NONA: A Tree Searching Program. Program and Documentation. www.cladistics.com/aboutNona.htm.

Harish, A., Caetano-Anollés, G., 2012. Ribosomal history reveals origins of modern protein synthesis. PLoS One 7, e32776.

Harpke, D., Peterson, A., 2008a. 5.8S motifs for the identification of pseudogenic ITS regions. Botany 86, 300–3005.

Harpke, D., Peterson, A., 2008b. Extensive 5.8S nrDNA polymorphism in *Mammillaria* (Cactaceae) with special reference to the identification of pseudogenic internal transcribed spacer regions. J. Plant Res. 121, 261–270.

Hasegawa, M., Kishino, H., Yano, T.-A., 1985. Dating of the human-ape splitting by a molecular clock of mitochondrial DNA. J. Mol. Evol. 22, 160–174.

Hershkovitz, M.A., Zimmer, E.A., Hahn, W.J., 1999. Ribosomal DNA sequences and angiosperm systematics. In: Hollingsworth, P.M., Bateman, R.M., Gornall, R.J. (Eds.), Molecular Systematics and Plant Evolution. Taylor & Francis, London, pp. 268–326.

Idžojtić, M., Pernar, R., Glavaš, M., Zebec, M., Diminić, D., 2008. The incidence of mistletoe (*Viscum album* ssp. *abietis*) on silver fir (*Abies alba*) in Croatia. Biologia 63, 81–85.

Karadžić, D., Lazarev, V., Milenković, M., 2004. The most significant parasitic and saprophytic fungi on common mistletoe (*Viscum album* L.) and their potential application in biocontrol. Bulletin Faculty of Forestry 89. University of Bajna Luka, Serbia, pp. 115–126.

Kauserund, H., Schumacher, T., 2003. Ribosomal DNA variation, recombination and inheritance in the basidiomycete *Trachaptum abietinum*: implications for reticulate evolution. Heredity 91, 163–172.

Keller, A., Schliecher, T., Fürster, F., Ruderisch, B., Dandekar, T., Müller, T., Wolf, M., 2008. ITS2 data corroborate a monophyletic chlorophycean DO-group (Sphaeropleales). BMC Evol. Biol. 8, 218.

Keller, A., Schleicher, T., Schultz, J., Müller, T., Dandekar, T., Wolf, M., 2009. rRNA interaction and HMM-based ITS2 annotation. Gene 430, 50–57.

Kluge, A.G., Farris, J.S., 1969. Quantitative phyletics and the evolution of Anurans. Syst. Zool. 18, 1–32.

Knudsen, V., Caetano-Anollés, G., 2008. NOBAI: a web server for character coding of geometrical and statistical features in RNA structure. Nucleic Acids Res. 36 (Suppl. 2), W85–W90.

Koetschan, C., Förster, F., Keller, A., Schleicher, T., Ruderisch, B., Schwarz, R., Müller, T., Wolf, M., Schultz, J., 2010. The ITS2 database III — sequences and structures for phylogeny. Nucleic Acids Res. 38, D275–D279.

Kovács, G.M., Balázs, T.K., Calonge, F.D., Martín, M.P., 2011. The diversity of *Terfezia* desert truffles: new species and a highly variable species complex with intrasporocarpic nrDNA ITS heterogeneity. Mycologia 103, 841–853.

Larkin, M., Blackshields, G., Brown, N., Chenna, R., McGettigan, P., McWilliam, H., Valentin, F., Wallace, I., Wilm, A., Lopez, R., et al., 2007. Clustal W and Clustal X version 2.0. Bioinformatics 23, 2947.

Li, Y., Jiao, L., Yao, Y.-J., 2013. Non-concerted ITS evolution in fungi, as revealed from the important medical fungus *Ophiocordyceps sinensis*. Mol. Phylogenet. Evol. 68, 373–379.

Lindner, D.L., Banik, M.T., 2011. Intragenomic variation in the ITS rDNA region obscures phylogenetic relationships and inflates estimates of operational taxonomic units in genus *Laetiporus*. Mycologia 103, 731–740.

Mai, J.C., Coleman, A.W., 1997. The internal transcribed spacer 2 exhibits a common secondary structure in green algae and flowering plants. J. Mol. Evol. 44, 258–271.

McBride, A.J.A., Cerqueira, G.M., Suchard, M.A., Moreira, A.N., Zuerner, R.L., Reis, M.G., Haake, D.A., Ko, A.I., Dellagostin, O.A., 2009. Genetic diversity of Leptospiral immunoglobulin-like (Lig) genes in pathogenic *Leptospira* spp. Infect. Genet. Evol. 9, 196–205.

Minin, V.N., Fang, F., Dorman, K.S., Suchard, M.A., 2005. Dual multiple change-point model leads to more accurate recombination detection. Bioinformatics 21, 3034–3042.

Müller, K., 2005. SeqState — primer design and sequence statistics for phylogenetic DNA data sets. Appl. Bioinforma. 4, 65–69.

Murat, C., Díez, J., Luis, P., Delaruelle, C., Dupré, C., Chevalier, G., Bonfante, P., Martin, F., 2004. Polymorphism at the ribosomal DNA ITS and its relation to postglacial recolonization routes of the Périgord truffle *Tuber melanosporum*. New Phytol. 164, 401–411.

Nabuurs, G.-J., Linder, M., Verkerk, P., Gunia, K., Deda, P., Michalak, R., Grassi, G., 2013. First signs of carbon sink saturation in European forest biomass. Nat. Clim. Change 3, 792–796.

Needleman, S.B., Wunsch, C.D., 1970. A general method applicable to the search for similarities in the amino acid sequence of two proteins. J. Mol. Biol. 48, 443–453.

Nickrent, D.L., Malécot, V., Vidal-Russell, R., Der, J.R., 2010. A revised classification of Santalales. Taxon 59, 538–558.

Nixon, K.C., 2002. Winclada. Version 1.00.08. www.cladistics.com/aboutWinc.htm (Ithaca, NY, USA).

Noetzli, K.P., Müller, B., Sieber, T.N., 2003. Impact of population dynamics of white mistletoe (*Viscum album* ssp. *abietis*) on European silver fir (*Abies alba*). Ann. For. Sci. 60, 773–779.

Nylander, J.A.A., Wilgenbusch, J.C., Warren, D.L., Swofford, D.L., 2008. AWTY (are we there yet?): a system for graphical exploration of MCMC convergence in Bayesian phylogenetics. Bioinformatics 24, 581–583.

O'Donnell, K., Cigelnik, E., 1997. Two divergent intragenomic rDNA ITS2 types within a monophyletic lineage of the fungus *Fusarium* are nonorthologous. Mol. Phylogenet. Evol. 7, 103–116.

Pan, Y., Birdsey, R.A., Fang, J., Houghton, R., Kauppi, P.E., Kurz, W.A., Phillips, O.L., Shvidenko, A., Lewis, S.L., Canadell, J.G., Ciais, P., Jackson, R.B., Pacala, S.W., McGuire, A.D., Piao, S., Rautiainen, A., Sitch, S., Hayes, D., 2011. A large and persistent carbon sink in the world's forests. Science 333, 988–993.

Phillips, A.J.L., Alves, A., Pennycook, S.R., Johnston, P.R., Ramaley, A., Akulov, A., Crous, P.W., 2008. Resolving the phylogenetic and taxonomic status of dark-spotted teleomorph genera in the *Botryosphaeriaceae*. Persoonia 21, 29–55.

Phillips, A.J.L., Alves, A., Abdollahzadeh, J., Slippers, B., Wingfield, M.J., Groenwald, J.Z., Crous, P.W., 2013. The *Botryosphaeriaceae*: genera and species known from culture. Stud. Mycol. 76, 51–167.

Poczai, P., Hyvönen, J., 2010. Nuclear ribosomal spacer regions in plant phylogenetics: problems and prospects. Mol. Biol. Rep. 37, 1897–1912.

Pöll, G., Braun, T., Jakovljevic, J., Neueder, A., Jakob, S., Woolford, J.L., Tschochner, H., Milkereit, P., 2009. rRNA maturation in yeast cells depleted of large ribosomal subunit proteins. PLoS One 4, e8249.

Rambaut, A., Drummond, A.J., 2012. Tracer v1.5. Available from. http://tree.bio.ed.ac.uk/software/tracer/.

Robert, V., Stegehuis, G., Stalpers, J., 2005. The MycoBank Engine and Related Databases. http://www.mycobank.org.

Ronquist, F., Teslenko, M., van der Mark, P., Ayres, D.L., Darling, A., Höhna, S., Larget, B., Liu, L., Suchard, M.A., Huelsenbeck, J.P., 2012. MrBayes 3.2: efficient Bayesian phylogenetic inference and model choice across a large model space. Syst. Biol. 61, 539–542.

Schoch, C.L., Seifert, K.A., Huhndorf, S., Robert, V., Spouge, J.L., Levesque, C.A., Chen, W., 2012. Nuclear ribosomal internal transcribed spacer (ITS) region as a universal DNA barcode marker for fungi. PNAS 109, 6241–6246.

Schultz, J., Maisel, S., Gerlach, D., Muller, T., Wolf, M., 2005. A common core of secondary structure of the internal transcribed spacer 2 (ITS2) throughout the eukaryota. RNA 11, 361–364.

Schultz, J., Müller, T., Achtziger, M., Seibel, P.N., Dandekar, T., Wolf, M., 2006. The internal transcribed spacer 2 database — a web based server for (not only) low level phylogenetic analyses. Nucleic Acids Res. 34, 704–707.

Seibel, P., Müller, T., Dandekar, T., Schultz, J., Wolf, M., 2006. 4SALE — a tool for synchronous RNA sequence and secondary structure alignment and editing. BMC Bioinforma. 7, 498.

Seibel, P., Müller, T., Dandekar, T., Wolf, M., 2008. Synchronous visual analysis and editing of RNA sequence and secondary structure alignments using 4SALE. BMC Res. Notes 1, 91.

Simmons, M.P., Ochoterena, H., 2000. Gaps as characters in sequence-based phylogenetic analyses. Syst. Biol. 49, 369–381.

Simon, U.K., Weiss, M., 2008. Intragenomic variation of fungal ribosomal genes is higher than previously thought. Mol. Biol. Evol. 25, 2251–2254.

Smith, M.E., Douhan, G.W., Rizzo, D.M., 2007. Intra-specific and intra-sporocarp ITS variation of ectomycorrhizal fungi as assessed by rDNA sequencing of sporocarps and pooled ectomycorrhizal roots from a *Quercus* woodland. Mycorrhiza 18, 15–22.

Stöver, B.C., Müller, K.F., 2010. TreeGraph 2: combining and visualizing evidence from different phylogenetic analyses. BMC Bioinforma. 11, 7.

Suchard, M.A., Weiss, R.E., Dorman, K.S., Sinsheimer, J.S., 2003. Inferring spatial phylogenetic variation along nucleotide sequences: a multiple change-point model. J. Am. Stat. Assoc. 98, 427–437.

Tamura, K., Peterson, D., Peterson, N., Stecher, G., Nei, M., Kumar, S., 2011. MEGA5: molecular evolutionary genetics analysis using maximum likelihood, evolutionary distance, and maximum parsimony methods. Mol. Biol. Evol. 28, 271–2739.

Tsopelas, P., Angelopoulos, A., Economou, A., Soulioti, N., 2004. Mistletoe (*Viscum album*) in the fir forest of Mount Parinis, Greece. For. Ecol. Manag. 202, 59–65.

Varga, I., 2013. The Distribution of European Mistletoe (*Viscum album*) in Hungary and Investigation of the Biological Control Potential of One of its Pathogen, *Phaeobotryosphaeria visci*. (PhD thesis). University of Pannonia, Keszthely, Hungary.

Varga, I., Taller, J., Baltazár, T., Hyvönen, J., Poczai, P., 2012. Leaf-spot disease on European mistletoe (*Viscum album*) caused by *Phaeobotryosphaeria visci*: a potential candidate for biological control. Biotechnol. Lett. 34, 1059–1065.

Varga, I., Poczai, P., Tiborcz, V., Aranyi, N.R., Baltazár, T., Bartha, D., Pejchal, M., Hyvönen, J., 2014. Changes in the distribution of the European mistletoe (*Viscum album* L.) in Hungary during the last hundred years. Folia Geobot. http://dx.doi.org/10.1007/s12224-014-9193-5.

Vargas, P., Morton, C., Jury, S.L., 1999. Biogeographic patterns in Mediterranean and Macaronesian species of *Saxifraga* (Saxifragaceae) inferred from phylogenetic analysis using ITS sequences. Am. J. Bot. 86, 724–734.

Venema, J., Tollervey, D., 1995. Processing of pre-ribosomal RNA in *Saccharomyces cerevisiae*. Yeast 11, 1629–1650.

White, T.J., Bruns, T., Lee, S., 1990. Amplification and direct sequencing of fungal ribosomal RNA genes for phylogenetics. In: Innis, M.A., Gelfand, H.D., Sninsky, J.J. (Eds.), PCR Protocol: A Guide to Methods and Applications. Academic Press, USA, pp. 315–322.

Wolf, M., Achtziger, M., Schultz, J., Dandekar, T., Müller, T., 2005. Homology modeling revealed more than 20,000 rRNA internal transcribed spacer 2 (ITS2) secondary structures. RNA 11, 1616–1623.

Yamaji, H., Fukuda, T., Yokoyama, J., Pak, J.-H., Zhou, C., Yang, C., Kondo, K., Morota, T., Takeda, S., Sasaki, H., Maki, M., 2007. Reticulate evolution and phylogeography in *Asarum* sect. *Asiasarum* (Aristolochiaceae) documented in internal transcribed specer sequences (ITS) of nuclear ribosomal DNA. Mol. Phylogenet. Evol. 44, 863–884.

Yao, H., Song, J., Liu, C., Luo, K., Han, J., Li, Y., Pang, X., Xu, H., Zhu, Y., Xiao, P., Chen, S., 2010. Use of ITS2 region as the universal DNA barcode for plants and animals. PLoS One 5, e13102.

Zhou, L.-W., Wei, Y.-L., 2012. Changbai wood-rotting fungi 16. A new species of *Fomitopsis* (Fomitopsidaceae). Mycol. Prog. 11, 435–441.

Zuber, D., 2004. Biological flora of Central Europe: *Viscum album* L. Flora 199, 181–203.